JPPIPA 9(6) (2023)

Jurnal Penelitian Pendidikan IPA

Journal of Research in Science Education

http://jppipa.unram.ac.id/index.php/jppipa/index

Synthesis and Characterization of Composites-Based Bacterial Cellulose by Ex-Situ Method as Separator Battery

Maria Ulfa[1*], Inda Noviani[1], Emmy Yuanita[1], Ni Komang Tri Dharmayani[1], Sudirman[1], Sarkono[2]

[1] Chemistry Department, Faculty of Mathematics and Natural Sciences, University of Mataram, Indonesia.
[2] Biology Department, Faculty of Mathematics and Natural Sciences, University of Mataram, Indonesia.

Received: April 15, 2023
Revised: May 9, 2023
Accepted: June 25, 2023
Published: June 30, 2023

Corresponding Author:
Maria Ulfa
ulfaarief@unram.ac.id

DOI: 10.29303/jppipa.v9i6.3819

Abstract: Many studies have been conducted and developed on cellulose-based battery separator materials, including bacterial cellulose, which has characteristics like plant cellulose. This research aims to synthesize BC/Al2O3 composite and analyze its potential as a battery separator. The synthesis of the composite with the ex-situ method is to immerse BC from tofu liquid waste (fermentation time variation of 6, 7, and 8 days) into Al2O3 suspension. The characterization results showed that the immersion of Al2O3 in BC can increase porosity, electrolyte absorption, and conductivity, indicating that the composite has the potential to be used as a battery separator.

Keywords: Battery separator; BC/Al_2O_3; Ex-situ; Tofu waste liquid

Introduction

The separator is a component part of the battery that functions as a separator between electrodes for the transfer of ions in the electrolyte and ensures that there is no short-circuit between the electrodes in the battery (Lee et al., 2018; Lu et al., 2018). Materials commonly used as commercial battery separators are based on polyolefins such as polypropylene (PP), polyethylene (PE), and tri-layer PP/PE/PP (Mun et al., 2021). However, there are some drawbacks, namely non-degradability, low porosity (36.31-44.00 %), electrolyte absorption, and low conductivity (Lee et al., 2018; Xu et al., 2017).

The search for separator materials has been extensive to address such weaknesses, and cellulose is one of the biopolymers that has been extensively studied as a separator battery because it has high porosity and affects ion conductivity (Ginting et al., 2023; Pan et al., 2019; Tanpichai et al., 2019; Wang et al., 2018; Xu et al., 2017; Zhu et al., 2021). Cellulose produced by bacteria, or bacterial cellulose (BC), has characteristics such as porosity, electrolyte absorption, conductivity, tension strength, and thickness that are not much different from the standard (Choi et al., 2022; Li et al., 2021; Muddasar et al., 2022; Xu et al., 2017), so it has the potential to be a separator battery (Ginting et al., 2023; Li et al., 2021; Qian et al., 2022).

The thickness and low tensile strength of the separator can affect battery safety (Hao et al., 2022). The selection of fermentation media used in the manufacture of BC greatly affects the thickness and tensile strength. The use of tofu and corn liquid waste media produces BC with a thickness 4-52 times greater than that of non-waste and is accompanied by low tensile strength (> 98.06 MPa) (Costa et al., 2019; Yasa et al., 2020). Several studies have conducted the addition of ceramic oxide-based fillers (SiO_2, Al_2O_3, TiO_2, and others) to overcome this weakness (Huy et al., 2021; Wei et al., 2019; Xu et al., 2017; Yu et al., 2021). The study by Xu et al. (2017), added

How to Cite:
Ulfa, M., Noviani, I., Yuanita, E., Dharmayani, N. K. T., Sudirman, & Sarkono. (2023). Synthesis and Characterization of Composites-Based Bacterial Cellulose by Ex-Situ Method as Separator Battery. *Jurnal Penelitian Pendidikan IPA*, *9*(6), 4647–4651. https://doi.org/10.29303/jppipa.v9i6.3819

$Al(NO_3)_3.9H_2O$ to BC with a simple in situ thermal decomposition method and produced BC/Al_2O_3 composites that have porosity, electrolyte absorption, thickness, tensile strength, and conductivity that can meet commercial separator standards.

According to the explanation above, the chemical and physical properties of BC and BC/Al_2O_3 composite were investigated to establish its potential as a separator battery. BC synthesis has been performed using Gluconacetobacter xylinus bacteria based on tofu liquid waste media, and BC/Al_2O_3 composite synthesis have been carried out ex-situ.

Method

Preparation of BC and BC/ Al_2O_3 composites

The production of BC in this study was carried out following the procedure used by Sarkono et al. (2014) with modifications. In this research, tofu liquid waste was used as a production medium, with nutrient compositions of 10.0, 0.5, and 0.5% (w/v) sugar, ammonium sulfate, and yeast extract in 100 mL production scale. The pH of the media was set to 5 and sterilized for 15 min in an autoclave at 121°C and 2 atm. The media were inoculated with coconut water-based starter culture (10% v/v) and static fermented for 6, 7, and 8 days at 30°C. BC hydrogels were harvested and cleaned with cold water to remove residual media before being boiled for approximately 15 min and soaked in 0.5 M NaOH for 24 h.

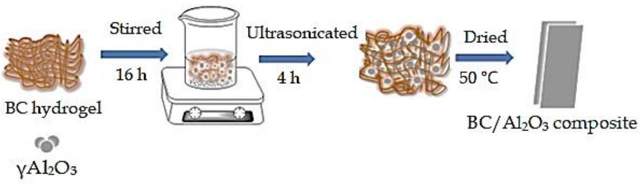

Figure 1. The schematic representation of a ex situ method to synthesize BC/Al_2O_3 composite

The water-reduced BC sheets were dried in an oven (50°C, 10 h). The dry BC was immersed into γ- Al_2O_3 suspension (1 g γ-Al_2O_3 in 1 L 0.8 M NaOH and stirred for 16 h) and ultrasonicat*ed* for 4 h and decanted to obtain γ- Al_2O_3 suspension (33 %), and dried in an oven (50 °C, 2 h).

Characterization

Chemical characterization of BC and BC/Al_2O_3 composites performed with FTIR-ATR and Raman (Bruker). Porosity was measured by immersing BC and BC/Al_2O_3 composites in *n*-butanol 80% (v/v) and calculated based on equation (1).

$$\phi = \frac{(M_b - M_k)}{\rho_B \ V_k} \times 100\ \% \quad (1)$$

where M_k and M_b are dry and wet mass of the sample, ρ_B is density *of n*-butanol (g/cm^3), and V_k is dry volume of the sample (cm^3). Electrolyte absorption was measured by immersing the sample in NaOH (1 M) electrolyte solution for 1 h and calculated using equation (2).

$$A_e = \frac{M_2 - M_1}{M_1} \times 100\ \% \quad (2)$$

where A_e is electrolyte absorption, M_1 and M_2 is sample mass before and after immersion. The conductivity of BC and BC/Al_2O_3 composites measured and calculated based on equation (3).

$$\sigma = \frac{1}{\rho} \quad (3)$$

where ρ is resistivity. Tensile strength is measured based on ASTM D638 with Tensilon RTG-1310 at load cell capacity 5.0 kN with a sampling rate of 5 mm/min. Composite surface morphology analysis using Scanning Electron Microscopy (FEI, Inspect-S50).

Result and Discussion

Figure 2 shows the FTIR-ATR spectra for BC and the BC/Al_2O_3 composite. Based on the absorption bands obtained, the spectra of BC and BC/Al_2O_3 composite have similarities with the difference in wavenumber magnitude as shown in Table 1. The difference in wave-number for reference BC with the research results as shown in Table 1., may be due to the base BC media used, where Galdino et al. (2020) and Güzel et al. (2019), using corn waste media, and orange peel.

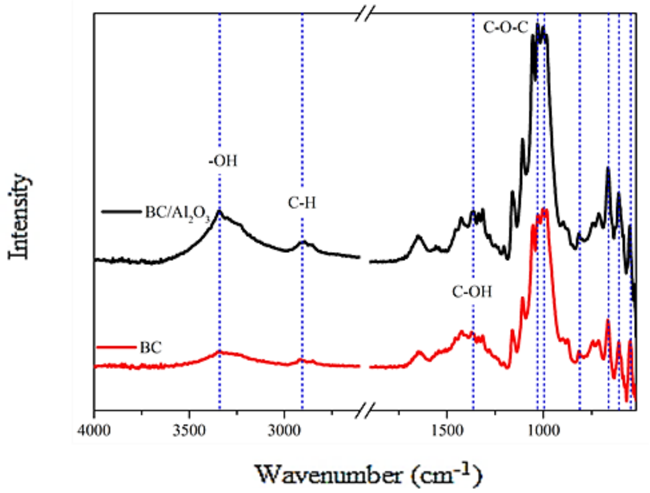

Figure 2. FTIR-ATR BC and BC/Al_2O_3 composite

A comparison of FTIR-ATR spectroscopy results from BC and BC/Al_2O_3 composites in Figure 2 shows the difference in the height and width of the absorption peaks of the two spectra. BC/Al_2O_3 composite do not show any difference in absorption at wavenumbers 881–558 cm^{-1} (confirms the existence of Al–O–Al vibrations) with the BC membrane (Atrak et al., 2018). The spectrum of the BC/Al_2O_3 composite displays a narrower peak compared to the spectrum from BC. This difference is made possible by the increased degree of crystallinity that occurs in the BC/Al_2O_3 composite. The increase in crystallinity causes molecular vibrations in the BC/Al_2O_3 composite more districts compared to BC. The increase in crystallinity was also caused by using ultrasonication in the Al_2O_3 dispersion process.

Table 1. Absorption Bands of FTIR-ATR BC and BC/Al_2O_3 Composites

Functional Groups	Wavenumber (cm^{-1}) Reference	BC	BC/Al_2O_3
O–H	3286[1];3270[2]; 3400–3440[2]	3348	3341
C–H	2921[1];1277[2]; 2800–2900[2]	2916	2893
C–OH	1399[1];1375[2]; 1440–1310[2]	1422	1361
C–O–C	1111[2]; 1040–1068[1]	1001	1027

[1] Galdino et al. (2020); [2] Guzel & Akpinar (2019)

Spectroscopy Raman was performed on BC and BC/Al_2O_3 composites to reconfirm the possibility of some vibrations not being recorded by the FTIR-ATR, with a maximum laser power of 50 mW. The spectrum results for the two composites are shown in Figure 2.

Spectroscopy Raman BC and BC/Al_2O_3 composites in Figure 3 shows the absorption with wavenumbers that are not much different. The vibrational region shows a similarity to the spectrum Raman for BC from aple cider waste media, with higher and narrower spectrum readings indicated by BC/Al_2O_3 composites.

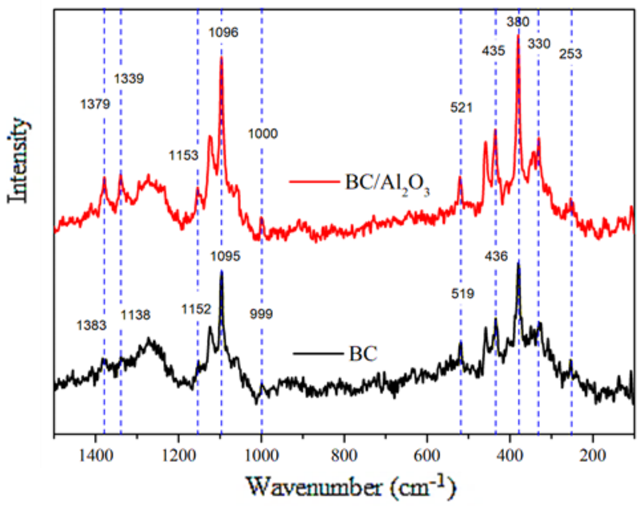

Figure 3. Spectral comparison Raman BC and BC/Al_2O_3 composites

Visualization of BC and BC/Al_2O_3 composites produced in this study gave a different appearance, namely in the form of transparent white sheets for BC and opaque white for BC/Al_2O_3 composites. This difference indicates the dispersed Al_2O_3 into BC at the time of fermentation for 6, 7, and 8 consecutive days at 14.00; 6.36; and 24.58% of 33.00% suspension-Al_2O_3.

Table 2. Porosity and Absorption of BC Electrolyte, BC/Al_2O_3 Composite, and Separators Standard

Fermentation Time (Days)	Porosity (%) BC	Porosity (%) BC/Al_2O_3	Electrolyte Absorption (%) BC	Electrolyte Absorption (%) BC/Al_2O_3
6	54.99	41.56	297.98	282.13
7	89.56	87.20	315.17	244.73
8	59.91	61.61	246.53	296.38
Separator Standard		51.2[1]		167[1]225[2]

[1] Wang et al. (2019); [2] Xu et al. (2017)

Porosity and electrolyte absorption test results on BC and BC/Al_2O_3 composites can be observed in Table 2. The porosity of BC and BC/Al_2O_3 composite for 7 days of fermentation is about 2 times higher than the standard separator, as well as the electrolyte absorption is higher than the standard. The existence of Al_2O_3 which dispersed the most in BC fiber at 8 days of fermentation (24.58%) resulted in greater absorption of electrolytes than without Al_2O_3, this is in line with the increased porosity of the BC/Al_2O_3 composite.

Table 3. Conductivity, Tensile Strength, and Thickness

Fermentation Time (Days)	Conductivity ($\times 10^{-4}$ S/cm)		Tensile Strength (MPa)		Thickness (μm)	
	BC	BC/Al_2O_3	BC	BC/Al_2O_3	BC	BC/Al_2O_3
6	0.340	2.460	102.92	85.72	25	37
7	0.129	0.519	121.87	93.92	32	35
8	0.251	2.02	166.08	82.301	28	45
Separator Standard	0.5[1]		58.1[1]		20[1]	

[1] Wang et al. (2019)

This increase is also influenced by the hydrophilicity of Al_2O_3, and properties of Al_2O_3 having moisture, wettability, and excellent electrolyte absorption (Xu et al., 2017). The separator must absorb and retain large amounts of liquid electrolyte to achieve low internal resistance and high ionic conductivity. The high tensile strength is also influenced by sonication during the dispersion of Al_2O_3 into BC fibers. This is because the use of prolonged ultrasonication increases the possibility of single BC fibers reacting with the microbubbles generated in the sonication process (acoustic cavitation effect), which can loosen the fiber surface and cause bond breakage to destroy the micro-sized microcrystalline cellulose fibers into nanocrystalline cellulose. The presence of Al_2O_3 through the dispersion process in BC fibers, can increase the thickness of BC/Al_2O_3 composites compared to BC (Fauza et al., 2019).

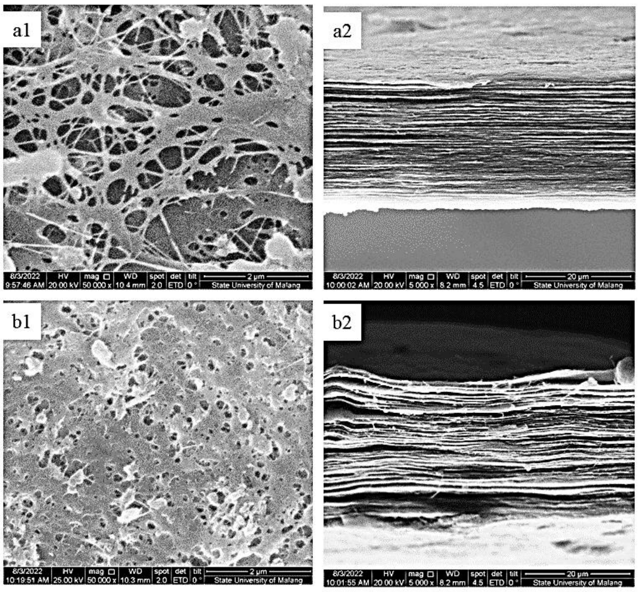

Figure 4. SEM image: a1. BC (50000×); a2. cross section of BC (5000×); b1. BC/Al_2O_3 composite (50000×); b2) Cross section of the BC/Al_2O_3 composite (5000×).

The surface morphology of BC and BC/Al_2O_3 composites gives a difference in fiber arrangement with an average BC fiber diameter of 65.59 nm. BC/Al_2O_3 Composite showed better crystallinity with Al_2O_3-coated fibers so that it shows a different visual from BC, this can be observed in the SEM image (Figure 4). BC/Al_2O_3 composite in the SEM image with cross sections shows cellulose fibers that are arranged in stacks but not as dense as the cellulose arrangement in BC, this is due to the presence of Al_2O_3 in BC fiber, as well as the sonication process during Al_2O_3 dispersion into the BC fiber which can loosen the BC fiber so that it provides a distance between the cellulose piles in the BC/Al_2O_3 composite. Morphological comparison of BC and BC/Al_2O_3 composites indicates that the dispersion of Al_2O_3 gives a change in the physical properties of BC.

Conclusion

BC/Al_2O_3 composite tofu liquid waste-based was successfully synthesized by ex-situ method through immersed Al_2O_3 in BC with variations in fermentation time. The crystallinity of the BC/Al_2O_3 composite has increased compared to BC, this can be observed in the FTIR-ATR and Raman spectra. The existence of Al_2O_3 in BC through the ex-situ method can increase the porosity, electrolyte absorption, and conductivity of BC/Al_2O_3 composite, so it can potentially be developed as a battery separator.

Acknowledgments

We thank our colleagues from State University of Malang (UM) and ITB for contributing SEM images and FTIR-ATR and Raman results, and the research team for working on this study.

Author Contributions

Maria Ulfa, and Sudirman organized and planned the research stages. Maria Ulfa, Sarkono and Inda Noviani carried out sample preparation and made BC and BC/Al_2O_3 composites and characterized the physical properties. Sudirman, Emmy Yuanita, and Ni Komang Tri Dharmayani contributed to data processing, analysis, and interpretation. Maria Ulfa led the manuscript writing. All authors actively provided feedback, and assisted in the research, data analysis and in writing the manuscript.

Funding

This research and APC are funded by the University of Mataram with PNBP (Non-Tax State Revenue) grants in 2023.

Conflicts of Interest

The authors declare no conflicts of interest. The funder had no role in the design of the study; in the collection, analysis, or interpretation of the data; in writing the manuscript; or in the decision to publish the results.

References

Atrak, K., Ramazani, A., F., T., & S. (2018). Green Synthesis of Amorphous and Gamma Aluminum Oxide Nanoparticles by Tragacanth Gel and Comparison of Their Photocatalytic Activity for The Degradation of Organic Dyes. *Journal of Materials Science: Materials in Electronics*, *29*(10), 8347–8353. https://doi.org/10.1007/s10854-018-8845-2

Choi, S. M., Rao, K. M., Zo, S. M., Shin, E. J., & Han, S. S. (2022). Bacterial Cellulose and Its Applications. *Polymers*, *14*(6), 1080. https://doi.org/10.3390/polym14061080

Costa, C. M., Lee, Y.-H., Kim, J.-H., Lee, S.-Y., & Lanceros-Méndez, S. (2019). Recent advances on separator membranes for lithium-ion battery applications: From porous membranes to solid electrolytes. *Energy Storage Materials*, *22*, 346–375. https://doi.org/10.1016/j.ensm.2019.07.024

Fauza, A. N., Mardiyati, M. M., & Steven, S. (2019). Pembuatan dan Karakterisasi Separator Baterai Berbahan Selulosa Alga Cladophora. *Jurnal Teknologi Bahan Dan Barang Teknik*, *9*(2), 69. https://doi.org/10.37209/jtbbt.v9i2.135

Galdino, C. J. S., Maia, A. D., Meira, H. M., Souza, T. C., Amorim, J. D. P., Almeida, F. C. G., Costa, A. F. S., & Sarubbo, L. A. (2020). Use of a bacterial cellulose filter for the removal of oil from wastewater. *Process Biochemistry*, *91*, 288–296.

https://doi.org/10.1016/j.procbio.2019.12.020

Ginting, D., Na Duma, T., Rahmadani, N., Suryani, Y., & Haryanti, R. (2023). Potential of Cellulose Acetat Separator of Empty Palm Oil Fruit Bunches and Polyvinylidene Fluoride for Energy Storage Applications. *POSITRON*, *13*(1), 51. https://doi.org/10.26418/positron.v13i1.63784

Güzel, M., & Akpınar, Ö. (2019). Production and Characterization of Bacterial Cellulose from Citrus Peels. *Waste and Biomass Valorization*, *10*(8), 2165–2175. https://doi.org/10.1007/s12649-018-0241-x

Hao, W., Bo, X., Xie, J., & Xu, T. (2022). Mechanical Properties of Macromolecular Separators for Lithium-Ion Batteries Based on Nanoindentation Experiment. *Polymers*, *14*(17), 3664. https://doi.org/10.3390/polym14173664

Huy, V. P. H., So, S., & Hur, J. (2021). Inorganic fillers in composite gel polymer electrolytes for high-performance lithium and non-lithium polymer batteries. *Nanomaterials*, *11*(3), 1–40. https://doi.org/10.3390/nano11030614

Lee, B.-S., Cui, S., Xing, X., Liu, H., Yue, X., Petrova, V., Lim, H.-D., Chen, R., & Liu, P. (2018). Dendrite Suppression Membranes for Rechargeable Zinc Batteries. *ACS Applied Materials & Interfaces*, *10*(45), 38928–38935. https://doi.org/10.1021/acsami.8b14022

Li, W., Wang, S., Fan, Z., Li, S., Bernussi, A., & Newman, N. (2021). Functionalized bacterial cellulose as a separator to address polysulfides shuttling in lithium–sulfur batteries. *Materials Today Energy*, *21*, 100813. https://doi.org/10.1016/j.mtener.2021.100813

Lu, W., Xie, C., Zhang, H., & Li, X. (2018). Inhibition of Zinc Dendrite Growth in Zinc-Based Batteries. *ChemSusChem*, *11*(23), 3996–4006. https://doi.org/10.1002/cssc.201801657

Muddasar, M., Beaucamp, A., Culebras, M., & Collins, M. N. (2022). Cellulose: Characteristics and applications for rechargeable batteries. *International Journal of Biological Macromolecules*, *219*, 788–803. https://doi.org/10.1016/j.ijbiomac.2022.08.026

Mun, S. C., & Won, J. H. (2021). Manufacturing Processes of Microporous Polyolefin Separators for Lithium-Ion Batteries and Correlations between Mechanical and Physical Properties. *Crystals*, *11*(9), 1013. https://doi.org/10.3390/cryst11091013

Pan, R., Sun, R., Wang, Z., Lindh, J., Edström, K., Strømme, M., & Nyholm, L. (2019). Double-sided conductive separators for lithium-metal batteries. *Energy Storage Materials*, *21*, 464–473. https://doi.org/10.1016/j.ensm.2019.06.025

Qian, J., Chen, Q., Hong, M., Xie, W., Jing, S., Bao, Y., Chen, G., Pang, Z., Hu, L., & Li, T. (2022). Toward stretchable batteries: 3D-printed deformable electrodes and separator enabled by nanocellulose. *Materials Today*, *54*, 18–26. https://doi.org/10.1016/j.mattod.2022.02.015

Sarkono, S., Moeljopawiro, S., Setiaji, B., & Sembiring, L. (2014). Physico-chemical Properties of Bacterial Cellulose Produced by Newly Strain Gluconacetobacter xylinus ANG-29 in Static and Shaking Fermentations. *Biosciences Biotechnology Research Asia*, *11*(3), 1259–1265. https://doi.org/10.13005/bbra/1514

Tanpichai, S., Witayakran, S., Srimarut, Y., Woraprayote, W., & Malila, Y. (2019). Porosity, density and mechanical properties of the paper of steam exploded bamboo microfibers controlled by nanofibrillated cellulose. *Journal of Materials Research and Technology*, *8*(4), 3612–3622. https://doi.org/10.1016/j.jmrt.2019.05.024

Wang, Z., Pan, R., Xu, C., Ruan, C., Edström, K., Strømme, M., & Nyholm, L. (2018). Conducting polymer paper-derived separators for lithium metal batteries. *Energy Storage Materials*, *13*, 283–292. https://doi.org/10.1016/j.ensm.2018.02.006

Wei, N., Hu, J., Zhang, M., He, J., & Ni, P. (2019). Cross-linked porous polymer separator using vinyl-modified aluminum oxide nanoparticles as cross-linker for lithium-ion batteries. *Electrochimica Acta*, *307*, 495–502. https://doi.org/10.1016/j.electacta.2019.04.010

Xu, Q., Wei, C., Fan, L., Peng, S., Xu, W., & Xu, J. (2017). A bacterial cellulose/Al2O3 nanofibrous composite membrane for a lithium-ion battery separator. *Cellulose*, *24*(4), 1889–1899. https://doi.org/10.1007/s10570-017-1225-x

Yasa, I. W. S., Basuki, E., Saloko, S., & Handito, D. (2020). Sifat Fisik dan Mekanis Lembaran Kering Selulosa Bakteri Berbahan Dasar Limbah Hasil Pertanian. *Jurnal Ilmiah Rekayasa Pertanian Dan Biosistem*, *8*(1), 89–99. https://doi.org/10.29303/jrpb.v8i1.170

Yu, X., & Manthiram, A. (2021). A review of composite polymer-ceramic electrolytes for lithium batteries. *Energy Storage Materials*, *34*, 282–300. https://doi.org/10.1016/j.ensm.2020.10.006

Zhu, C., Zhang, J., Qiu, S., Jia, Y., Wang, L., & Wang, H. (2021). Tailoring the pore size of polyphenylene sulfide nonwoven with bacterial cellulose (BC) for heat-resistant and high-wettability separator in lithium-ion battery. *Composites Communications*, *24*, 100659. https://doi.org/10.1016/j.coco.2021.100659